Phys. Status Solidi B **248**, No. 12, 2921–2926 (2011) / **DOI** 10.1002/pssb.201147075

physica status solidi b
www.pss-b.com
basic solid state physics

Comparing study of magnetic-ion and nonmagnetic-ion doping effect at Mn site in $La_{0.825}Sr_{0.175}MnO_3$ compound

Changyi Hao[1], Bangchuan Zhao*[,2], Guangli Kuang[1], and Yuping Sun[1,2]

[1] High Magnetic Field Laboratory, Chinese Academy of Sciences, Hefei 230031, P.R. China
[2] Key Laboratory of Materials Physics, Institute of Solid State Physics, Chinese Academy of Sciences, Hefei 230031, P.R. China

Received 15 February 2011, revised 5 May 2011, accepted 5 May 2011
Published online 2 June 2011

Keywords doping, LaSrMnO, magnetic properties, phase transitions, structure, transport

* Corresponding author: e-mail bchzhao@issp.ac.cn, Phone: +86 551 559 1439, Fax: +86 551 599 1434

Structural, magnetic, and transport properties of $La_{0.825}Sr_{0.175}MnO_3$ samples doped with magnetic (Fe^{3+}, Cr^{3+}) and nonmagnetic (Ga^{3+}, Al^{3+}) ions have been studied comparatively. The structure does not change by nonmagnetic ion doping, whereas magnetic ion substitution can change the structure of the system significantly. All the doped samples show a lower Curie temperature as compared to that of the undoped sample. The change of Curie temperature T_C for the magnetic-ion-doped samples is quite larger than that of the nonmagnetic-ion-doped samples. The electron configuration is suggested to play an important role in determining the change of T_C for the magnetic-ion-doped samples, whereas the decrease of T_C in nonmagnetic-doped samples is considered to originate mainly from the variation of local lattice. The Fe-doped sample shows semiconducting transport behavior in the whole studied temperature range besides a kink near T_C. Except for two obvious M–I transitions, another inflexion-like anomaly in the $\rho(T)$ curve at low temperatures is observed for the Ga-, Cr-, and Al-doped samples and the inflexion is suggested to be related to a two transport channel model in these samples.

1 Introduction Colossal magnetoresistance (CMR) manganites with a general formula $Re_{1-x}A_xMnO_3$ (Re = rare-earth ions, A = divalent ions) have been a subject of intensive research in view of their special electronic and magnetic properties as well as their potential applications [1–6]. It is commonly believed now that the double-exchange (DE) interaction proposed by Zener [7] plays an essential role to realize the nature of the CMR effect. When a fraction of the rare-earth ions Re^{3+} is substituted by a divalent ion A^{2+}, a proportional number of Mn^{3+} ions is converted to Mn^{4+} ions and mobile e_g electrons can be introduced, mediating the ferromagnetic (FM) interaction between Mn^{3+} and Mn^{4+} ions. In order to stabilize the low temperature DE interaction and then the FM metallic phase, a hole doping level x in the range of 0.2–0.5 is needed and the optimum value of x is 0.33. However, calculations to account for large changes in resistivity within this framework did not yield a satisfactory result. Additional ingredients such as lattice distortion, electron correlation, and orbital degree of freedom should be considered to interpret the large field and temperature dependence of resistivity observed in experiments [8].

Among the most studied manganite oxides, $La_{1-x}Sr_xMnO_3$ has the maximum one-electron bandwidth W at the doping level of $x \sim 0.3$. The magnetic and electrical phase diagrams of the system are more complicated due to the subtle interplay of spin, charge, orbital, and lattice degrees of freedom in the system [9]. The parent compound $LaMnO_3$ exhibits an A-type antiferromagnetic (AFM) spin state below a certain temperature $T_N = 120$ K. With the substitution of Sr for La in the doping level $x < 0.1$, the low temperature A-type AFM phase changes to the spin-canted AFM phase. A FM insulator along with charge/orbit ordering (CO/OO) will appear for strontium concentrations in the level of $0.1 \leq x \leq 0.17$. As the Sr-doping level increases further, the magnetic and transport behavior of the system becomes FM and metallic below the Curie temperature (T_C). The stable FM metallic phases persist up to almost half doping level of strontium. In order to clarify the mechanism of the CMR effect in $La_{1-x}Sr_xMnO_3$, various elements, such as Fe, Cr, Ga, Al, Ti, Cu, and Ru [10–16], are selected to substitute for Mn in the system due to the crucial role of Mn ions in the material. Most experiments reveal that the Mn site

doping will weaken the long-range FM ordering resulting in the decrease of Curie temperature. Moreover, magnetic and nonmagnetic ions doping at Mn sites always have a different effect [17]. It should be noted that the previous Mn-site doping works have mainly focused on FM metallic compounds such as $La_{0.7}Sr_{0.3}MnO_3$. Studies on the element substitution effect in the AFM phase or critical state between FM and AFM phase are still lacking [15]. In order to comprehensively understand the Mn-site doping effect in these materials, we carefully investigate the effect of both magnetic (Fe, Cr) and nonmagnetic (Al, Ga) ions doping in the critical compound $La_{0.825}Sr_{0.175}Mn_{0.95}X_{0.05}O_3$ at a fixed doping level $x = 0.05$ (X = Mn, Fe, Cr, Al, and Ga). To simplify the description, hereafter, the Mn-, Fe-, Cr-, Al-, and Ga-doped samples are abbreviated as LSMO, LSMFO, LSMCO, LSMAO, and LSMGO, respectively.

2 Experimental $La_{0.825}Sr_{0.175}Mn_{0.95}X_{0.05}O_3$ (X = Mn, Fe, Cr, Ga, and Al) polycrystalline samples were synthesized by conventional solid-state reaction method. Appropriate high purity powders La_2O_3 (99.99%), $SrCO_3$ (99.9%), MnO_2 (99.95%), and $Fe_2O_3/Cr_2O_3/Ga_2O_3/Al_2O_3$ (99.9%) were thoroughly mixed and pre-heated in air at 900 °C for 10 h. The obtained powders were ground, pelletized, and sintered at 1000 °C for 10 h, 1200 and 1400 °C for 20 h with intermediate grinding, then the furnace was cooled down to room temperature. The structural characterization was examined by powder X-ray diffraction (XRD) using CuKα radiation at room temperature. The temperature dependence of the resistance was measured by the standard four-probe method from 5 to 380 K under 0 and 5 T magnetic fields on a commercial Quantum Design physical property measurement system (PPMS) ($1.8\,K \le T \le 400\,K$, $0\,T \le H \le 9\,T$). The magnetic measurements were performed on a Quantum Design superconducting quantum interference device (SQUID) MPMS system ($1.8\,K \le T \le 400\,K$, $0\,T \le H \le 5\,T$).

3 Results and discussion Figure 1 shows the powder XRD patterns of $La_{0.825}Sr_{0.175}Mn_{0.95}X_{0.05}O_3$ (X = Mn, Fe, Cr, Ga, and Al) samples at room temperature. The XRD shows that all the studied samples are single phase with no detectable impurity materials and the samples had a distorted perovskite structure. Moreover, the XRD patterns of the nonmagnetic-ion- and undoped LSMGO, LSMAO, and LSMO samples can be well indexed by a rhombohedral lattice with space group $R\bar{3}C$, whereas XRD patterns of the magnetic-ion-doped LSMFO and LSMCO samples can be described by the mixed phases of rhombohedral lattice ($R\bar{3}C$) and orthorhombic lattice (*Pnma*). The rhombohedral phases are 18.56 and 13.1% for the Fe- and Cr-doped samples, respectively. The structural parameters can be obtained by fitting the experimental spectra using the standard Rietveld technique. The obtained structural parameters along with the fitting parameter R_p are shown in Table 1. Previous reports show that 5% Fe or Cr substitution for Mn in the FM metallic compound of $La_{0.7}Sr_{0.3}MnO_3$ does not change the crystal structure of the system due to the similar ionic radii of Fe^{3+}, Cr^{3+}, and Mn^{3+} ions [10–12]. However, our results indicate that Mn-site doping in the critical compound $La_{0.825}Sr_{0.175}MnO_3$ has a complicated behavior. Magnetic ions Fe^{3+} and Cr^{3+} doping change the lattice from rhombohedral to the mixed phase rhombohedral ($R\bar{3}C$) and orthorhombic (*Pnma*), where the orthorhombic phase is dominating phase. The nonmagnetic-ion doped samples LSMAO and LSMGO have the same crystal structure with the undoped sample LSMO. It is stated that the lattice

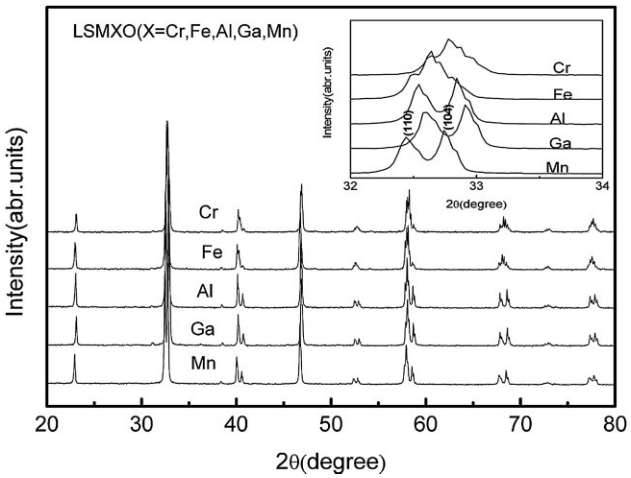

Figure 1 Room temperature XRD pattern for $La_{0.825}Sr_{0.175}Mn_{0.95}X_{0.05}O_3$ (X = Mn, Ga, Al, Fe and Cr). The inset shows the enlarged view in the diffraction angle range of $32° \le 2\theta \le 34°$.

Table 1 Ionic and electron configuration (EC) of X^{3+} ions; space group (SG), lattice structure, cell parameters, and unit cell volumes for $La_{0.825}Sr_{0.175}Mn_{0.95}X_{0.05}O_3$ (R: $R\bar{3}C$; O: *Pnma*).

X	r_x (Å)	EC	SG	a (Å)	b (Å)	c (Å)	V (Å^3)
Mn^{3+}	0.645	$t_{2g}^3 e_g^1$	R	5.537	5.537	13.376	355.16
Fe^{3+}	0.645	$t_{2g}^3 e_g^2$	R (18.56%)	5.534	5.534	13.360	354.38
			O (81.44%)	5.505	7.797	5.544	237.97
Cr^{3+}	0.615	$t_{2g}^3 e_g^0$	R (13.1%)	5.543	5.543	13.377	355.94
			O (86.9%)	5.505	7.796	5.546	238.02
Ga^{3+}	0.62	$3d^{10}$	R	5.544	5.544	13.386	356.33
Al^{3+}	0.535	[Ne]	R	5.538	5.538	13.376	355.32

parameters of the samples doped with nonmagnetic ions are slightly larger than that of the undoped samples, though Al^{3+} and Ga^{3+} ions have a smaller ionic radius than that of Mn^{3+}. The results are contrary to the Ga-doped $La_{2/3}Sr_{1/3}MnO_3$ compound, where the lattice shrinks as Ga ions are added to the sample [13].

The inset of Fig. 1 shows the enlarged view of the XRD patterns in the 2θ range of 32–34°. It is evident that LSMO, LSMGO, and LSMAO display double peaks (110)/(104) near 32.5°, while only a single peak can be observed in the magnetic-ion-doped samples LSMFO and LSMCO at the same 2θ position, indicating the occurrence of the structural transformation in these two samples. It should be noted that the parent compound $La_{0.825}Sr_{0.175}MnO_3$ used in this work is located in the critical boundary of the FM metallic phase and PM insulating phase at room temperature [9]. The fragile balance can be easily destroyed and then structural transformation can occur in these materials by an external perturbation such as magnetic field [18, 19]. Actually, structural transformation induced by external magnetic field has been observed indeed in $La_{0.83}Sr_{0.17}MnO_3$ by Asamitsu et al. [19]. Besides external perturbation, our results demonstrate that magnetic element substitution at the Mn site can also cause a structural transformation in these critical $La_{1-x}Sr_xMnO_3$ compounds.

The temperature dependence of the magnetization M under an applied magnetic field of 0.01 T at field-cooling (FC) mode is shown in Fig. 2 for all $La_{0.825}Sr_{0.175}Mn_{0.95}X_{0.05}O_3$ samples. All the studied samples show an obvious PM–FM phase transition at corresponding Curie temperature T_C (defined as the inflection point of the M–T curve). For the undoped sample LSMO, the value of T_C (281 K) is consistent with the result reported previously. Both magnetic- and nonmagnetic-ion-doped samples show a lower Curie temperature as compared to that of the undoped sample. The value of T_C shifts to lower temperature gradually as the dopant changes from Ga to Al, then Cr and Fe. The result shows that the variation of T_C for the doped samples is closely related to the magnetic state and the ionic radius of the dopant ions. In order to illuminate the relationship of change of T_C and ionic radius of the dopant quantitatively, the Δr dependence of ΔT_C is plotted in Fig. 3, where Δr and ΔT_C are defined as $\Delta r = r(Mn^{3+}) - r(X^{3+})$ and $\Delta T_C = T_C(Mn) - T_C(X)$, respectively. It is shown that ΔT_C has an almost inverse change trend with that of Δr. The Fe-doped sample has the largest ΔT_C of about 70 K, though Fe^{3+} ion has the same ionic radius as Mn^{3+} (0.645 Å), whereas the value of ΔT_C is quite smaller for the Ga- and Al-doped samples. That is to say, magnetic ion doping has a more notable effect on T_C in the present system than the doping effect with nonmagnetic ions. The result can be explained by the combined effect of the difference of electron configuration and ionic radius between X^{3+} and Mn^{3+} ions in the samples. According to the DE theory, the decrease of T_C arises from a weak overlap between Mn-3d and O-2p orbitals, leading to a weakening of carrier bandwidth (W) of the e_g band. An empirical formula $W = W_0(\cos\theta/2)d^{3.5}$ can be usually used to describe the noted dependence, where W_0, θ, and d are the matrix element depending on the overlap between the neighboring orbitals, the Mn–O–Mn bond angle and the average Mn–O bond distance respectively. The change of W_0 (defined as E-factor) or Mn–O–Mn angle and Mn–O distance (defined as S-factor) will change the DE process, leading to the change of Curie temperature T_C [17]. Both E- and S-factor in present samples have a negative effect on T_C and the effect of E-factor is stronger than that of S-factor. In the magnetic-ion-doped samples, the E-factor plays a more important role in determining T_C than the S-factor leading to much larger ΔT_C in these samples. However, T_C of the nonmagnetic-ion-doped samples is mainly affected by the S-factor, so T_C of the nonmagnetic-ion-doped samples is closer to the undoped samples as compared to the magnetic-ion-doped samples.

The magnetization as a function of the magnetic field $M(H)$ at 5 K is shown in Fig. 4. The magnetization reaches saturation at about 0.5 T and almost keeps constant up to 4.5 T for all samples, which is considered as a result of the rotation of the magnetic domain under external magnetic

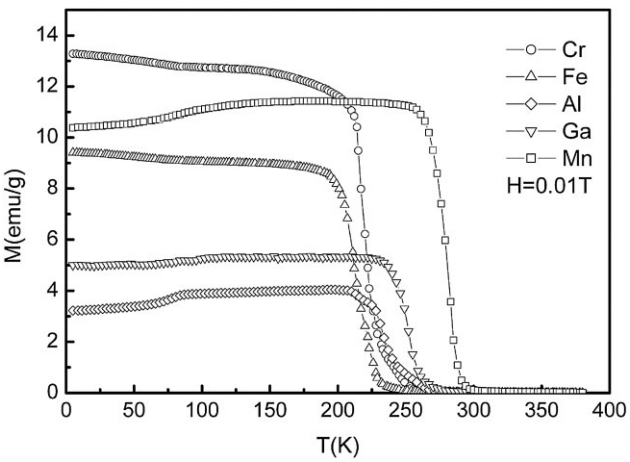

Figure 2 Temperature dependence of magnetization for LSMXO samples measured at 0.01 T field under FC mode.

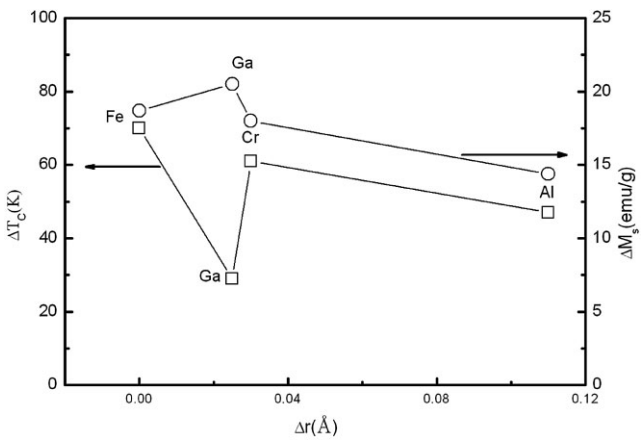

Figure 3 The relation between $\Delta M_S = M_S(Mn) - M_S(X)$, $\Delta T_C = T_C(Mn) - T_C(X)$, and $\Delta r = r(Mn^{3+}) - r(X^{3+})$.

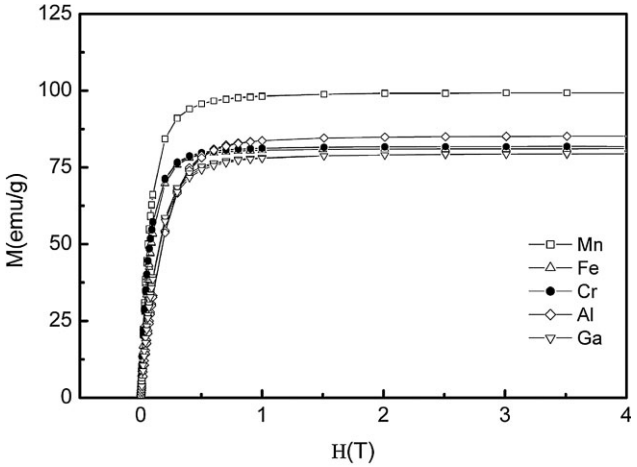

Figure 4 Field dependence of magnetization for LSMXO compounds measured at 5 K.

field. The result shows that both magnetic and nonmagnetic ions doping in present work do not change the FM ground state of LSMO. From the M (H) curve we can deduce the saturation magnetization M_S of the samples. All the element-substituted samples show a lower saturation magnetization as compared to those without substitution. From the figure we can see that doping with 5% magnetic as well as nonmagnetic ions results in a reduction of saturation magnetization of about 20%, which is practically independent on the doped ions. This is difficult to explain in terms of a reduced DE interaction by slightly changed lattice parameters as aforementioned. It seems that the inserted ions (including magnetic and nonmagnetic ions) locally suppress the DE interaction in favor of a super-exchange driven AFM alignment of the spins around the doped ions, which may be the origin of the observed reduction of the saturation magnetization because it clearly exceeds the reduction expected from the doping level. In order to study the doping effect on M_S by different ions, the variation of M_S (defined as $\Delta M_S = M_S(\mathrm{Mn}) - M_S(\mathrm{X})$) as function of Δr is shown in Fig. 3. The variation of M_S for the doped samples has a similar change trend with that of T_C except for the Ga-doped sample. The Ga-doped sample has the largest ΔM_S among the four element-substituted samples, whereas its ΔT_C is the smallest. Moreover, from Fig. 3 we can see that the discrepancy of the effect on M_S between magnetic ion doping and nonmagnetic ion doping is not such remarkable as the effect on T_C.

In order to investigate the Mn-site doping effect on the transport properties of the studied samples, the temperature dependence of resistivity $\rho(T)$ is measured in the temperature range of 5–380 K at zero magnetic field. The resistive results are shown in Fig. 5a–e for the un-, Ga-, Al-, Fe-, and Cr-doped samples. For the undoped sample LSMO, an obvious insulator–metal (I–M) phase transition at $T_{p1} \sim 279$ K is observed in the $\rho(T)$ curve, which is close to its corresponding T_C. The $\rho(T)$ curve in the low temperature metallic region below T_{p1} can be well fitted using the formula $\rho = \rho_0 + AT^{2.5}$, implying that the low temperature electric transport of the sample is dominated by magnon-carrier scattering mechanism [15]. When partially Mn ions were substituted, the transport behavior of the system becomes more complicated. An I–M transition can also be observed in the Ga-, Cr-, and Al-doped samples, but the transition temperature T_{p1} decreases significantly as compared to the undoped sample. The value of T_{p1} is 218, 223, and 228 K for the samples doped with Ga, Cr, and Al, respectively, which are listed in Table 2. As temperature decreases from T_{p1}, ρ decreases and reaches a minimum value till to a certain temperature (defined as T_{p2}), then increases slowly again. The value of T_{p2} is also listed in Table 2. In the low temperature semiconducting region, another inflexion at T^*

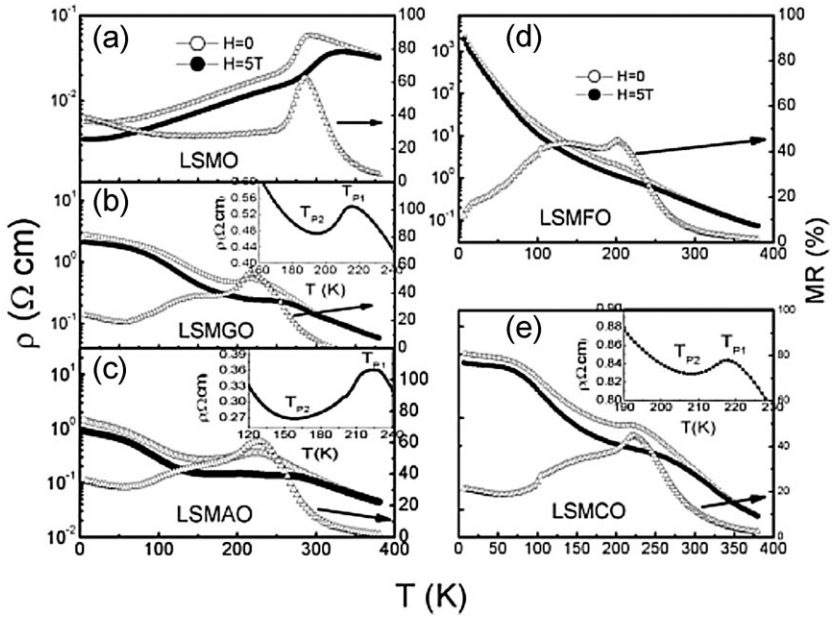

Figure 5 The temperature dependence of resistivity under 0 and 5 T field and MR vs. T curves for LSMO (a), LSMGO (b), LSMAO (c), LSMFO (d), and LSMCO (e) samples. The insets of (b), (c), and (e) show the enlarged view of ρ–T curves for LSMGO, LSMAO, and LSMCO, respectively.

Table 2 The fitting parameters and critical temperature T^* at 0 and 5 T field; the I–M transition temperature (T_{p1}) and M–I transition temperature (T_{p2}) for LSMGO, LSMAO, and LSMCO compounds.

parameters	LSMGO		LSMAO		LSMCO	
	0 T	5 T	0 T	5 T	0 T	5 T
ρ_{11} (Ω cm)	2.589	2.174	1.735	0.899	5.093	3.996
A (Ω cm K$^{-1.5}$)	0.0123	0.0072	0.0067	0.0043	0.0110	0.0064
ρ_{21} (Ω cm)	—	—	—	—	0.0826	0.0436
ρ_{22} (Ω cm)	0.0386	0.0297	0.141	0.034	—	—
T_{21} (K)	—	—	—	—	466.4	480.4
T_{22} (K)	2448.2	1963.5	890.5	1227.9	—	—
T^* (K)	87.5	74.5	56.1	58.5	74.4	73.0
T_{p1} (K)	217.6		215.3		224.5	
T_{p2} (K)	208.2		195.7		158.7	

is observed on the $\rho(T)$ curve. We think that the inflexion on the $\rho(T)$ curve of LSMCO, LSMGO, and LSMAO is probably caused by the formation of two transport channels in the materials as discussed below. As to the Fe-doped sample LSMFO, ρ increases continuously with decreasing temperature besides a small kink near T_C. Previous studies have shown that Mn^{3+} in LSMO can be easily substituted by Fe^{3+} ions at low Fe doping level [19, 20]. Mössbauer spectroscopy [21] demonstrates that the Fe ion usually couples antiferromagnetically with its Mn neighbors. The large value of ΔT_C and variation of resistivity in LSMFO compared to the undoped sample in the present work may be related to the appearance of local AFM order between Fe^{3+} and its neighboring Mn ions. 5% Fe substitution in $La_{0.825}Sr_{0.175}MnO_3$ is sufficient to destroy the metallic state below T_C, the result is contrary to the situation of Fe-doping effect at Mn site in the optimum-doping $La_{0.7}Sr_{0.3}MnO_3$ compound.

The temperature dependence of resistivity $\rho(T)$ is also measured under an applied magnetic field of 5 T for all studied samples, the result is also plotted in Fig. 5. It shows that the resistivity of the samples decreases under the applied magnetic field, T_{p1} peak position shifts to a higher temperature and T_{p2} position shifts to a lower temperature. The magnetoresistance (MR) as a function of temperature based on the measured data is also plotted in Fig. 5. Here MR is defined as $MR = [\rho(0) - \rho(5T)]/\rho(0)$, where $\rho(0)$ is the resistivity at zero field and $\rho(5T)$ is the resistivity under 5 T. There are obvious MR peaks in the vicinity of T_{p1} in the $MR(T)$ curves of all samples. However, the field effect on T^* is distinct for different element doped samples. For the Cr- and Ga-doped samples, T^* shifts to lower temperature under the applied magnetic field, whereas T^* shifts to higher temperature for LSMAO. Moreover, the $MR(T)$ curve exhibits a local minimum near T^* for LSMCO, LSMGO and LSMAO samples. To understand the inflexion at T^* deeply, we try to fit the low-temperature $\rho(T)$ curve near the inflexion using different models (thermally activated conduction law, a variable range hopping model and the polaron-hopping model [22, 23]) and found the $\rho(T)$ curve can be well described as the following formula:

$$\rho(T) = \frac{\rho_1 \rho_2}{\rho_1 + \rho_2}. \quad (1)$$

Here $\rho_1 = \rho_{11} + AT^{2.5}$ represents the resistivity of the metallic transport channel, $\rho_2 = \rho_{21}\exp(T_{21}/T)$ for Cr-doped sample, and $\rho_2 = \rho_{22}\exp(T_{22}/T)^{1/4}$ for Ga- and Al-doped samples represent the resistivity of the semiconducting transport channel. The fitting results for the Ga-, Al-, and Cr-doped samples are shown in Fig. 6a–c, respectively. That is to say, there exist two transport channels in the materials: one is metallic and the other is semiconducting-like. As discussed above, the inserted ions will locally suppress

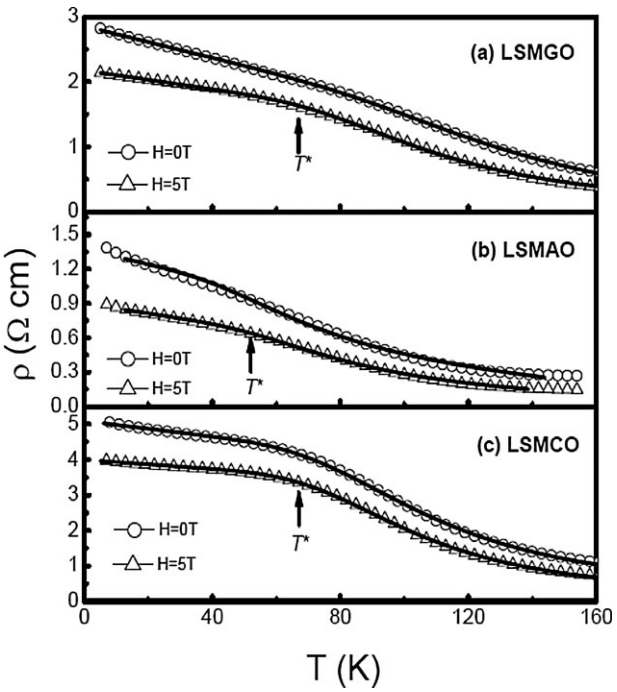

Figure 6 The temperature dependence of resistivity under 0 and 5 T fields for LSMGO (a), LSMAO (b), and LSMCO (c) samples at low temperatures. The open symbols represent experimental data and the lines are the calculated curves according to Eq. (1).

the DE interaction around the impurity and the electron hopping between adjacent Mn ions. Therefore, the resistivity increases and the transport becomes semiconducting-like as the doped ions were inserted. However, the doping level was quite low and the metallic transport channel was preserved. The combined effect of the two channels results in the appearance of the inflexion at T^* in the $\rho(T)$ curves. From the fitting, we can see that the transport properties in the semiconducting channel of the samples doped with magnetic ions is activated behavior, whereas the transport properties of the sample doped with nonmagnetic ions can be well described by a variable range hopping model. The disorder effect may play an import role in the transport properties of these samples doped with nonmagnetic ions.

4 Conclusion In summary, the effect of magnetic and nonmagnetic ion doping at the Mn site on the structural, magnetic, and electronic properties of $La_{0.825}Sr_{0.175}Mn_{0.95}X_{0.05}O_3$ (X = Mn, Ga, Al, Fe, and Cr) compounds is investigated. It is found that the structure of $La_{0.825}Sr_{0.175}Mn_{0.95}X_{0.05}O_3$ is sensitive to the magnetic properties of the doped ions. An obvious structural transition was found in the magnetic-ion-doped samples LSMFO and LSMCO. The decrease of T_C caused by magnetic and nonmagnetic ions has different physical origin. The E-factor is suggested to play an important role in determining the change of T_C for the magnetic-ion-doped samples LSMFO and LSMCO, whereas the decrease of T_C in the nonmagnetic-doped samples is considered to originate mainly from the S-factor. Two obvious M–I transition are observed in the $\rho(T)$ curve of the Ga-, Cr-, and Al-doped samples. In addition, the $\rho(T)$ curve of these samples shows an inflexion in the low-temperature range below 100 K. The result is suggested to be related to a two transport channel model in these Mn-site-doped samples.

Acknowledgements This work was supported by the Nature Science Foundation of Anhui Province of China under Contract No. 090414184 and the National Nature Science Foundation of China under Contract No. 10374033.

References

[1] R. von Helmolt, J. Wecker, B. Holzapfel, L. Schultz, and K. Samwer, Phys. Rev. Lett. **71**, 2331 (1993).
[2] S. Jin, T. H. Tiefel, M. McCormack, R. A. Fastnacht, R. Ramesh, and L. H. Chen, Science **264**, 413 (1994).
[3] A. Urushibara, Y. Moritomo, T. Arima, A. Asamitsu, G. Kido, and Y. Tokura, Phys. Rev. B **51**, 14103 (1995).
[4] Y. Tokura, A. Urushibara, Y. Moritomo, T. Arima, A. Asamitsu, G. Kido, and N. Furukawa, J. Phys. Soc. Jpn. **63**, 3931 (1994).
[5] B. Dabrowski, X. Xiong, Z. Bukowski, R. Dybzinski, P. W. Klamut, J. E. Siewenie, O. Chmaissem, J. Shaffer, C. W. Kimball, J. D. Jorgensen, and S. Short, Phys. Rev. B **60**, 7006 (1999).
[6] O. Chmaissem, B. Dabrowski, S. Kolesnik, J. Mais, J. D. Jorgensen, and S. Short, Phys. Rev. B **67**, 094431 (2003).
[7] C. Zener, Phys. Rev. **82**, 403 (1951).
[8] A. J. Millis, P. B. Littlewood, and B. I. Shraiman, Phys. Rev. Lett. **74**, 5144 (1995).
[9] J. Hemberger, A. Krimmel, T. Kurz, H. A. Krug von Nidda, V. Y. Ivanov, A. A. Mukhin, A. M. Balbashov, and A. Loidl, Phys. Rev. B **66**, 094410 (2002).
[10] M. M. Xavier, F. A. O. Cabral, A. de Uacute, J. H. Jo, C. Chesman, and T. Dumelow, Phys. Rev. B **63**, 012408 (2000).
[11] W. X. Xianyu, B. H. Li, Z. N. Qian, and H. M. Jin, J. Appl. Phys. **86**, 5164 (1999).
[12] Y. Sun, W. Tong, X. J. Xu, and Y. H. Zhang, Appl. Phys. Lett. **78**, 643 (2001).
[13] J. Blasco, J. Garcia, J. Stankiewicz, Phys. Rev. B **68**, 054421 (2003).
[14] D. N. H. Nam, L. V. Bau, N. V. Khiem, N. V. Dai, L. V. Hong, N. X. Phuc, R. S. Newrock, and P. Nordblad, Phys. Rev. B **73**, 184430 (2006).
[15] L. Pi, L. Zheng, and Y. Zhang, Phys. Rev. B **61**, 8917 (2000).
[16] Y. Ying, J. Y. Fan, L. Pi, Z. Qu, W. Q. Wang, B. Hong, S. Tan, and Y. H. Zhang, Phys. Rev. B **74**, 144433 (2006).
[17] A. N. Ulyanov, J. S. Kim, G. M. Shin, K. J. Song, Y. M. Kang, and S. I. Yoo, Physica B **388**, 16 (2007).
[18] E. S. Itskevich, V. F. Kraidenov, and S. M. Kuzmin, J. Low Temp. Phys. **32**, 928 (2006).
[19] A. Asamitsu, Y. Moritomo, Y. Tomioka, T. Arima, and Y. Tokura, Nature **373**, 407 (1995).
[20] G. H. Jonker, Physica **20**, 1118 (1954).
[21] A. Simopoulos, M. Pissas, G. Kallias, E. Devlin, N. Moutis, I. Panagiotopoulos, D. Niarchos, C. Christides, and R. Sonntag, Phys. Rev. B **59**, 1263 (1999).
[22] M. Ziese and C. Srinitiwarawong, Phys. Rev. B **58**, 11519 (1998).
[23] A. Seeger, P. Lunkenheimer, J. Hemberger, A. A. Mukhin, V. Y. Ivanov, A. M. Balbashov, and A. Loidl, J. Phys.: Condens. Matter **11**, 3273 (1999).

